5.12 VERIFICATION OF HELLENIC NATIONAL METEOROLOGICAL SERVICE HIGH RESOLUTION MM5 FORECASTS DURING THE 2004 ATHENS OLYMPIC GAMES

J. M. Henderson [*], T. S. Zaccheo
Atmospheric and Environmental Research, Inc.,
Lexington, MA, USA 02421

I. Pytharoulis
Meteognosis S.A., Zarifi 6, Nea Smirni 17124, Greece [†]

1. Introduction

The weather service of the host country of the Olympic Games is responsible for providing meteorological guidance to event planners and the public. As such, weather observations and forecasts for the 2004 Summer Olympic Games were provided by the Hellenic National Meteorological Service (HNMS). Atmospheric and Environmental Research, Inc. (AER) provided HNMS with a standalone nowcasting system that complemented the existing forecasting facilities with rapid updates to short-term forecasts of surface fields out to 6 h. The nowcasting system included a statistical technique for advecting satellite and radar imagery out to one hour. The radar imagery was generated by a newly-installed Doppler radar that was part of a larger infrastructure upgrade at HNMS.

Timely forecasts of sensible surface weather is especially relevant to an outdoor sporting event of the scope of the Olympic Games. Thousands of athletes and spectators are susceptible to extreme weather conditions, including, but not limited to, thunderstorms, hail, tornadoes, high temperatures and high heat stress levels. Coordinated activites in the past have focussed on the ability to observe and predict these weather events of importance. The Forecast Demonstration Project held during the Sydney 2000 Olympics (May et al. 2004) provided insight into many aspects of operational nowcasting systems, including both benefits and difficulties associated with system implementation, operational performance, data dissemination techniques and communication, training, verification and other logistical demands. The nowcasting system discussed in this paper is one such example of a self-contained forecasting package that involves data assimilation and NWP for short-term forecasts of 0-6 h, as well as a correlation-based technique for advecting existing radar and satellite images out to 1 h. This paper briefly describes the NWP and data assimilation techniques, the implementation configuration, and objective verification of selected fields. An example is then presented which subjectively evaluates the MM5 forecast fields. Approximately 500 MM5 simulations were generated during the 42 days between 2 August and 12 September 2004 (inclusive) [hereafter, the Olympic Games Period (OGP)]. These simulations form the basis of this study, which, it is hoped, makes a useful contribution to the long-term objective verification of high-resolution NWP. It is noted that the high frequency of the runs (every 2 h) decreases the likelihood of independence between individual model runs.

2. The Weather of Athens

a. Summer Climate

The temperature, relative humidity and precipitation fields exhibit large spatiotemporal variability over Greece (Zabakas 1981; Flokas 1994). In the warm period of the year (July-September), southern Europe and the Mediterranean region are mainly influenced by high-pressure resulting from the extension of the subtropical anticyclone of the Azores into the mid-latitudes. Differential heating between the warm land and the cooler sea is an additional factor that contributes to the existence of high-pressure in the area (Kallos et al. 1998). These conditions decrease the number of transient low-pressure centers in the Mediterranean region during the summer. Katsoulis and Kanteres (1979) have shown that the most favourable period of the year for the occurrence of fine weather in

[*]Corresponding author: J. M. Henderson, Atmospheric and Environmental Research, Inc., 131 Hartwell Avenue, Lexington, MA 02421. e-mail: jhenders@aer.com

[†]Current affiliation: HNMS, El. Venizelou 14, Helliniko 16777, Athens, Greece

Table 1: Summary statistics for Hellenikon for August and September 2004 based on 3-hourly synoptic reports. Temperature and dew point are in degrees Celsius and wind speed is in ms^{-1} .

Month	Mean T	Max T	Min T	Max Td	Min Td	Mean wind speed	Max wind speed
August	27.1	33.0	19.8	23.8	9.6	2.2	10.0
September	23.9	32.8	13.2	21.9	2.9	2.4	9.0

Greece is between 9 and 29 August.

Following Varinou (2000), the prevailing synoptic conditions over the Attica peninsula during the warm period of the year are: a) Etesians: These are generally northerly winds blowing over the eastern Mediterranean between mid-May and mid-October and are associated with stable weather conditions, clear skies, low relative humidity and lack of precipitation. Their formation is related to the westward extension of the Anatolian low together with the existence of high-pressure over southern Europe and the Balkan peninsula. In the Attica region, the Etesians induce a northeasterly flow. The winds strengthen just before noon and weaken during the night and early morning, allowing the formation of local thermal circulations. The mean monthly frequency of days with Etesians in Greece is 43% in August and 17% in September. b) Weak synoptic flow dominated by thermal circulations: High pressure prevails over the Mediterranean and southern Europe, resulting in weak pressure gradients and the development of land-sea breezes. On the west coast of Attica, southwesterly sea breezes from the Saronic Gulf typically do not exceed 5 ms^{-1} . The mean monthly frequency of sea-breeze days in Greece is 28% in August and 23% in September. Timing the strength and interaction of these winds with the local orography is a significant forecast problem for the water-based Olympic events.

Typical of the Athens urban area, the August mean conditions at Hellenikon (Kornaros 1999) are a temperature of 27.8 C, a north wind of 4.0 ms^{-1} , 7.0 mm of precipitation and 1.8 days of rain. For September, the mean conditions are a temperature of 24.2 C, a north wind of 3.6 ms^{-1} , 9.6 mm of rain and 3.9 rainy days. In Attica, summers are dry and hot with infrequent thunderstorm activity. Of special concern for the Olympic Games' organizers are extreme daytime temperatures. For all months of August and September from 1955 to 1998 contained in the GDCN database (NCDC 2002), the Hellenikon observing site experienced maximum temperatures between 15.2 and 41.9 C, and minimum temperatures between 10.4 to 30.4 C. A higher temperature (44.8 C) has been observed elsewhere in the greater Athens area at Nea Philadelfia, while a temperature of 45.2 C has been measured at Larisa in central Greece. The stressing effects on humans of these extreme daytime temperatures are exacerbated in urban areas by lower wind speeds. During summer, central and southern continental Greece, Attica and Crete are the warmest areas while the Aegean and the Ionian Sea are relatively cooler. The spatial distribution of precipitation over Greece depends significantly on topography. Attica and the Saronic Gulf are characterized by small precipitation amounts, especially during summer. At Hellenikon from 1955 to 1998 (NCDC 2002), the maximum daily precipitation was 70.2 mm, with 94.9 % of the days having no observed precipitation and only 1.4 % of days having more than 5 mm of rain.

b. Weather during August and September 2004

Synoptic observations every 3 h from Hellenikon suggest relatively quiescent conditions in Attica during the months of August and September 2004. No precipitation was recorded during the two months (note that there are several missing observations). Summary statistics in Table 1 indicate that average temperatures and wind speeds for the two months were comparable to the long-term normals. No extremely high temperatures were recorded and dew point temperatures were not excessive.

Figure 1 and Fig. 2 show the location of observation sites in Greece and the Attica peninsula, respectively, for which forecast evaluation statistics are presented later in the paper. (Note that these two figures correspond to modelling domains 2 and 4, respectively, of the MM5; see the next section for more information on the MM5 and Fig. 4 for how domain 4 is positioned wrt domain 2). HNMS installed a network of 20 mesonet stations in Attica designed to provide high temporal and spatial-resolution observations close to the Olympic venues. There are 54 sites in domain 2 of which 36 are available on the GTS circuit and 18 are mesonet sites in Attica. These same eighteen mesonet sites are also located in domain 4 (DAFN and HELN are omitted). Two GTS sites (LGTT and LGAT) are also located in domain 4. The mean 2-m temperature, 2-m dew point temperature and 10-m wind speed (Fig. 3) were computed from all observations during the OGP that are valid at the top of each hour. Temperatures exhibit

a dependence on elevation and are warmest in the urban centers, while dew point decreases with elevation and distance from the warm ocean environment. Wind speeds are noticeably higher for sites exposed to the predominantly north and northeast wind and are lower in sheltered urban areas.

3. System configuration

a. Overview of system

The nowcasting system was installed on four nodes of an HPUX cluster at HNMS headquarters in Hellenikon, Greece. Each nowcast was designed to complete within 2 h, thus providing forecasters with new forecast fields 12 times daily. The nowcasting system was fully automated and was comprised of the following: observation ingest and quality control, preprocessing of NWP grids for ingest into 3d-VAR, integration of the MM5 model, postprocessing of NWP grids (including output of GRIB-format files) and posting to the web of graphical output.

b. MM5 details

The non-hydrostatic, fully compressible, regional Penn State/MM5 atmospheric modelling system is described by Dudhia (1993). It is widely used in the research community due, in part, to the open-source nature of its development that has resulted in a large choice of physical parameterizations.

The MM5 - as configured to run at HNMS - used 31 vertical sigma levels up to 100 hPa and quadruply-nested domains of dimension 115x115 (d1), 100x100 (d2), 52x52 (d3) and 61x61 (d4). Figure 4 shows the nested domain configuration of the MM5 in the nowcasting system. The outermost domain satisifes the option of using ECMWF "frames" data and allowed placement of the lateral boundary conditions far from the region of interest (Greece and, especially, the Attica peninsula). Domain 2 was designed to cover the entire country of Greece, while domain 4 provided coverage over all mainland Olympic venues.

The grid spacing of the domains (27, 9, 3 and 1 km) was chosen to allow resolvable scales down to 3-5 km on the innermost domain. As such, mesoscale details can be resolved in the low-level wind, temperature and moisture fields that are strongly forced by orography, proximity to water bodies and the urban heat island effect. Wind fields in the Athens metropolitan area are modified by Mt. Parnitha (1400 m) to the north, Mt. Penteli (1100 m) to the northeast and Mt. Hymettus (1050 m) to the east. To the immediate southwest of the city is the Saronic Gulf and its influence on sea breezes.

Following Kotroni and Lagouvardos (2001, 2004), the following model parameterizations were used: Kain-Fritsch (Kain and Fritsch 1993) cumulus convection, Schultz (1995) explicit microphysics, Hong and Pan (1996) PBL scheme and the AER-developed RRTM longwave radiation scheme (Mlawer et al. 1997). It should be noted that the Kain-Fritsch and Schultz schemes produced less precipitation than the other combinations of parameterizations for the cold season cases of Kotroni and Lagouvardos (2001). Sensitivity tests by the authors were not possible due to time constraints.

No cumulus parameterization scheme was used on the 3- and 1-km domains in an attempt to encourage the explicit development of convection. We note that the ability of the innermost domains to develop explicit convection can be heavily influenced by the presence and choice of parameterized convection schemes on the coarser-resolution domains (Warner and Hsu 2000; Colle et al. 2003). Two-way nesting was used for all domains to allow high-resolution features on the innermost domains to contribute to the flow patterns on the outer domains. The anticipation is that while sub 10-km grid spacing may not increase objective skill scores (Mass et al. 2002), forecasters may benefit from the presence of more realistic small-scale features.

c. 3d-VAR basics and configuration

The standard MM5 3d-VAR package (Barker et al. 2003) was implemented at HNMS to provide improved initial conditions and lateral boundary conditions for each subsequent MM5 simulation. In general terms, MM5 3d-VAR attempts to minimize the following cost function:

$$J(x) = J_b + J_o \tag{1}$$

$$= \frac{1}{2}(x-x^b)^T B^{-1}(x-x^b) \tag{2}$$

$$+\frac{1}{2}(y-y^o)^T (E+F)^{-1}(y-y^o) \tag{3}$$

The goal is to find an analysis x representing the minimum variance estimate of the true (unknown) state of the atmosphere given the *a priori* previous forecast x^b and a set of observations y^o. The fit is constrained through the background (B), observation instrument (E) and observation representative (F) error covariance matrices. The gridded background field is interpolated to the location of the observations as part of the 3d-VAR preprocessing step

Table 2: Extremes of temperature, dew point temperature and wind speed based on all observations and model forecasts during the OGP that are valid at the top of each hour. Temperature and dew point are in degrees Celsius and wind speed is in ms^{-1} .

Domain/ type	Max T	Min T	Max Td	Min Td	Max wind speed
d2 obs	40.9	3.9	29.9	-16.2	21.6
d2 forecasts	36.3	2.5	26.4	-1.1	17.4
d4 obs	37.9	11.9	23.9	-1.2	19.6
d4 forecasts	38.0	10.6	27.0	5.8	19.2

and extensive quality control of the observations is undertaken to remove duplicate, erroneous or out-of-domain observations.

During the OGP reported here, surface-based (SYNOP and METARS) and upper-air (RAWINSONDE) observations, as well as a number of surface mesonet locations from around the Attica peninsula, were presented to 3d-VAR on domain 1. Typically several hundred observations were available for each 3d-VAR analysis on the outermost domain, however, this number increased when rawinsonde observations were available every 12 h. All observations within a 90-minute window of the analysis time were ingested into the 3d-VAR observation preprocessor. As is common practice, hydrometeor fields were not included in the 3d-VAR analysis.

Background error statistics appropriate for mesoscale forecast background fields were used instead of the large-scale statistics supplied with the MM5 3d-VAR distribution. These statistics were derived from a month-long dataset of mesoscale (30-km grid spacing) forecasts using the NMC method and were provided by Francois Vandenberghe of NCAR (personal communication, 2004).

As noted by Mass et al. (2002), the use of densely-spaced mesonet observations may be required to define the small-scale temperature and moisture details needed for explicit convection in a weakly forced environment. The 27-km grid spacing for these analyses, however, may preclude the best use of these observations in 3d-VAR, since the mesonet observations are located entirely within the very small areal extent of domain 4. Thus, in domain 1, they are effectively treated as a single composite observation.

Application of 3d-VAR was limited to domain 1 for several reasons. Most importantly, background error statistics were only available for grid scales of approximately 30 km. Resource limitations, plus a lack of timely data, also placed restrictions on the ability to apply 3d-VAR on other domains.

d. Forecast fields

The following fields were available every 15 min: 2-m temperature and dew point, 10-m vector wind field, 2-m heat index (Rothsfusz 1990), wind speed and gusts, relative humidity, 15-min QPF, precipitation type, visibility, and flow streamlines. An example (Fig. 5) of the innermost domain temperature and wind field, valid the afternoon before the opening ceremonies of the 2004 Olympic Games, shows the complex surface wind flow, including sea breezes and interaction with the orography of the Attica peninsula. Of note in the temperature field are the high temperatures associated with the urban land surface characteristics of Athens and the dependence on elevation.

e. Forecast schedule

The nowcasting system was started 12 times daily at approximately 0040, 0240, ..., 2240 UTC. This permitted accumulation of observations valid at the top of the hour for immediate use in the 3d-VAR analysis valid at 0000 UTC, 0200 UTC. etc. ECMWF model grids, appropriately interpolated in time to account for a 12-h delay (wrt the ECWMF model's initial time) in receipt, formed the background field for the 3d-VAR analysis at 0000 and 1200 UTC. For other analysis times, the previous 2-h MM5 forecast field was used. Forecast fields from hours 2 through 8 of the subsequent MM5 simulation were available to forecasters via a web-based graphical display just after the valid time of the 2-h forecast.

4. Forecast evaluation

MM5 forecasts of temperature, dew point and wind speed from the OGP were compared against observations valid at the top of the hour (Mesonet observations were often available every 10 minutes). To convert to local time, add 2 h to UTC. The MM5 dataset included forecast fields from 504 simulations initialized every 2 h and with forecast lengths every hour from 2 h through 8 h. Fore-

Table 3: Statistics for temperature, dew point temperature and wind speed based on all observations during the OGP that are valid at the top of each hour. All sites in each domain are used unless otherwise noted. Temperature and dew point temperature are in degrees Celsius and wind speed in ms^{-1} .

Domain	Field	Sites	Bias	Stdev
d2	T	all	-1.3	2.1
d2	T	d4	-1.2	1.9
d4	T	d4	-1.0	1.8
d2	Td	all	2.0	3.2
d2	Td	d4	2.9	3.0
d4	Td	d4	2.9	2.9
d2	wind speed	all	0.8	2.8
d2	wind speed	d4	0.3	2.6
d4	wind speed	d4	0.8	2.7

cast lengths less than 2 h were not included to allow the general spinup of hydrometeor fields, as well as the formation of realistic mesoscale features. The closest grid point to the observation location was used. In a few instances, comparison of a marine grid point with an observation may result in substantially different verification statistics. It should be noted that the temperature and dew point observations were only available rounded to the nearest whole degree Celsius. They were then converted to integer Kelvin units. Precipitation forecasts were not verified because observed precipitation amounts were unavailable. However, as noted earlier, the verification period over Attica was largely precipitation-free. The Athens-city observation site Thissio, in addition to the above-mentioned Hellenikon site, recorded zero precipitation for the months of August and September.

As a gross evaluation, the OGP extrema of observed and forecast temperature, dew point and wind speed (Table 2), indicate reasonable agreement. Of note in domain 2 are the very low dew point temperature that are not well modelled and the very high observed dew points.

a. Summary statistics

Table 3 shows mean forecast errors (forecast minus observed) for temperature, dew point and wind speed. The forecasts exhibit sufficiently small bias that forecasters are provided useful information. The magnitude of the temperature forecast errors, and the presence of the negative bias, are similar to those reported by Kotroni and Lagouvardos (2004), though their longer forecast lengths are noted. The sample size is large (d2 more than 117000 comparisons; d4 more than 43000), lending support to the robustness of the values. Domain 2 temperature forecasts are too low on average, while dew point forecasts are too high (forecast too moist). Wind speed forecasts are slightly too high. A comparison of d4 forecasts with d2 forecasts for the same cities shows that increasing the grid spacing to 1 km from 9 km does not systematically improve forecasts among the three variables. Indeed, wind speed forecasts are degraded, while temperature forecasts improve slightly. This is a common result seen in the literature (Mass et al. 2002). Of interest is the increase in forecast bias of dew point temperature in d4 versus d2 forecasts using all d2 sites. This suggests perhaps that the spatial variability of moisture is higher among the d4 sites than the d2 sites and thus potentially more difficult to simulate. Note that the locations and times of the forecast-observation pairs that comprise the top two comparisons in Table 3 are identical, except for a processing error that affected archiving of the data on 26 August. As a result, an inconsequential number of extra comparisons (35 out of 43577) were included for the d2 comparison involving only the d4 sites.

1) Domain 2 - Greece The d2 temperature forecast bias by city (Fig. 6a, Fig. 7a, and Fig. 8a) is generally negative and increases with forecast length. Only LTBU has a noticeable positive bias.

Similar plots for dew point temperature (Fig. 6b, Fig. 7b, and Fig. 8b) indicate a positive bias in which the model overpredicts the moisture content. There is no increase in bias with increased forecast length and the magnitude of the bias is larger than for temperature. The largest forecast errors – exceeding 4 C at all forecast lengths – occur for observation locations in the interior of the Attica peninsula. Outliers in which the bias is notably negative include LATI and LWOH in the northwest part of mainland Greece. It should be noted that during the summer months the troposphere is generally dry in Greece, except for a shallow surface moist layer provided by local bodies of water. The shallow extent of the surface moist layer can be seen in the 1200 UTC 18 August sounding from Hellenikon (Figure 9). Lapse rates are also super-adiabatic at the surface, which indicates strong surface heating. Any differences between the model and true elevation will exacerbate any modelled errors in the synoptic pattern overlaid by the land-sea circulations.

The sign of the wind speed bias (Fig. 6c, Fig. 7c, and Fig. 8c) is inconsistent among all cities in domain 2, though the overall bias is positive. Interestingly, the trend at many sites is for a decrease in bias with increasing forecast length.

When binned by the model initial time (not shown) for

all 12 daily forecasts (0000 UTC, 0200 UTC, etc.), there does not appear to be a change in forecast statistics for the "cold start" 0000 and 1200 UTC model runs in which new coarse resolution ECMWF grids replace the high-resolution grids from the previous MM5 forecast as the background field in 3d-VAR. Competing factors include a negative impact due to the loss of mesoscale detail or a positive impact due to the inclusion of more recent boundary conditions provided by the ECWMF model.

A strong diurnal cycle is evident in the forecast bias by observation valid time (Fig. 10). The dearth of overnight observations interupts the diurnal trend in forecast errors. For temperature, the smallest mean errors occur for forecasts verifying during the nighttime hours (1900-0400 UTC), with forecasts during the time of peak heating verifying the poorest. For dew point temperature, forecast errors are at a minimum between 0300 and 0800 UTC, while the sign of the wind speed errors changes from positive to negative from 0800 to 1400 UTC. Perhaps the MM5 is deficient at modelling the strong daytime mixing that occurred with almost daily full solar insolation, with resulting wind speeds that are too low and temperatures that are too cool. Indeed, as can be seen in Figure 9, superadiabatic lapse rates occur during the summer. Poorly modelled surface mixing in the presence of moist surface air and dry air aloft may also account for errors in surface dew point forecasts.

2) Domain 4 - Attica The domain 4 temperature forecast bias by station (Fig. 11a) is again entirely negative and increases with increasing forecast length – except for KOTR. Dew point temperature forecast errors (Fig. 11b) exhibit a similar pattern to those of domain 2, with the largest biases again restricted to inland stations. Wind speed errors (Fig. 11c) are more strongly positively biased, with only 2 of 20 stations having a negative bias (AIGI and LAVR).

The diurnal cycle is also present in a plot of forecast error by valid time of the observations (Figure 12) and exhibits similar characteristics to domain 2. Of note is the less peaked diurnal cycle in temperature errors in which relatively large errors occur from early morning through to the time of the largest errors in the early afternoon.

b. Example of spurious convection

This small-scale dry thunderstorm outflow (see moisture and wind fields in Fig. 13) feature is an example of spurious convection that did not verify, however, it did develop on a day in which convection developed in other parts of Attica. The ability of the MM5 to highlight at least the possibility of convection in domain 4 suggests some value to forecasters, despite not being able to pinpoint the timing and location.

5. Conclusion

In this paper we introduce the MM5-based nowcasting system that was incorporated into the daily operations at the Hellenic National Meteorological Service in time for the 2004 Athens Olympic Games. Modified initial conditions for the MM5 are created with 3d-VAR 12 times daily using either ECMWF or cycled MM5 fields as the background inputs. Then quadruply-nested high-resolution MM5 model forecasts are produced for hours 2 through 8. For a 42-day period in August and early September, including the Olympic Games in the second half of August, verification statistics have been computed for temperature, dew point and wind speed. In general, forecast errors are sufficiently small that the NWP forecasts provided useful information to the forecasters. Temperature forecasts generally were too low, while forecasts of dew point temperature were too high. Wind speed forecasts overall were too high, though were too low from late morning through mid afternoon. These errors may be influenced by many factors, some common to Greece. They included: land-sea boundaries; a dry boundary layer except for a very shallow moist layer originating from water bodies; differences in model vs true orography; and the smoothing effect on low-level moisture of 3d-VAR when applied on a 27-km grid spacing. It is hoped that this paper satisfies, in part, the ongoing need for verification of high-resolution NWP forecasts over long periods of time.

These results support improvements suggested in the literature: applying 3d-VAR or 4d-VAR at higher resolution, more extensive mesonet observations, attention to improving NWP prediction of convection and additional verification of high-resolution NWP forecasts over long time periods.

6. References

Barker, D. M., W. Huang, Y.-R. Guo, A. J. Bourgeois and Q. N. Xiao, 2004: A Three-Dimensional Variational Data Assimilation System for MM5: Implementation and Initial Results. *Mon. Wea. Rev.*, **132**, 897-914.

Colle, B. A., J. B. Olson and J. S. Tongue, 2003: Multiseason Verification of the MM5. Part II: Evaluation of High-Resolution Precipitation Forecasts over the Northeastern United States, *Wea. Forecasting*, **18**, 458-480.

Dudhia, J., 1993: A Nonhydrostatic Version of the Penn State/NCAR Mesoscale Model: Validation Tests and Simulation of an Atlantic Cyclone and Cold Front. *Mon. Wea. Rev.*, **121**, 1493-1513

Flocas, A. A., 1994: A Course in Meteorology and Climatology. Zitis Press, Thessaloniki, Greece, 465 pp.

Hong, S-Y. and H-L. Pan, 1996: Nonlocal Boundary Layer Vertical Diffusion in a Medium-Range Forecast Model. *Mon. Wea. Rev.*, **124**, 2322-2339.

Kain, J. S. and J. M. Fritsch, 1993. Convective Parameterisation for Mesoscale Models: The Kain-Fritsch Scheme. In: The representation of cumulus convection in numerical models. Eds: K.A. Emanuel and D. J. Raymond. AMS Monograph, **46**, pp. 246.

Kallos, G., Kotroni V., Lagouvardos K. and Papadopoulos A., 1998. On the long range transport of air pollutants from Europe to Africa. *Geophys. Res. Lett.*, **25**, 619-622

Katsoulis, V. and N. Kanteres, 1979: Probabilities of fine weather in Greece. Hellenic National Meteorological Service, publication series, no.6

Kotroni, V. and K. Lagouvardos, 2004: Evaluation of MM5 High-Resolution Real-Time Forecasts over the Urban Area of Athens, Greece. J. of Appl. Met., **43**, 1666-1678.

___ and ___, 2001: Precipitation forecast skill of different convective parameterization and microphysical schemes: application for the cold season over Greece, *Geophys. Res. Lett.*, **28**, 1977-1980.

Mass, C. F., D. Ovens, K. Westrick and B. A. Colle. 2002: Does Increasing Horizontal Resolution Produce More Skillful Forecasts?, *Bull. Amer. Meteor. Soc.*, **83**, 407-430.

May, P. T., T. D. Keenan, R. Potts, J. W. Wilson, R. Webb, A. Treloar, E. Spark, S. Lawrence, E. Ebert, J. Bally and P. Joe, 2004: The Sydney 2000 Olympic Games Forecast Demonstration Project: Forecasting, Observing Network Infrastructure, and Data Processing Issues, *Wea. Forecasting*, **19**, 115-130.

Mlawer, E. J., S. J. Taubman, P. D. Brown, M. J. Iacono, and S. A. Clough, 1997: Radiative transfer for inhomogeneous atmospheres: RRTM, a validated correlated-k model for the longwave, *J. Geophys. Res.*, **102(D14)**, 16663-16682.

NCDC, 2002: The Global Daily Climatology Network (GDCN). Version 1.0, Climate Analysis Branch. [Available online at http://www.ncdc.noaa.gov/gdcn.html.]

Rothfusz, L. P., 1990: The heat index equation (or, more than you ever wanted to know about heat index). /NWS Southern Region Technical Attachment, SR/SSD 90-23,/ Fort Worth, TX. ¡http://www.nwstulsa.noaa.gov/mic_mesg0798.html¿

Schultz, P., 1995: An Explicit Cloud Physics Parameterization for Operational Numerical Weather Prediction. *Mon. Wea. Rev.*, **123**, 11, 3331-3343.

Warner, T. T. and H-M. Hsu, 2000: Nested-Model Simulation of Moist Convection: The Impact of Coarse-Grid Parameterized Convection on Fine-Grid Resolved Convection, *Mon. Wea. Rev.*, **128**, 2211-2231.

Varinou, M., 2000: Characteristic scales of dispersion and photochemical transformation of air pollutants in the region of northeastern Mediterranean. Ph.D. Thesis, Univ. of Athens, Greece.

Zabakas I.D., 1981. General Climatology. Athina Press, Athens, Greece, 493 pp.

Fig. 1: *Locations of observations in domain 2 for which statistics have been computed. Note that observation locations that also are located in domain 4 (see Fig. 4) are plotted only in Fig. 2 to preserve legibility.*

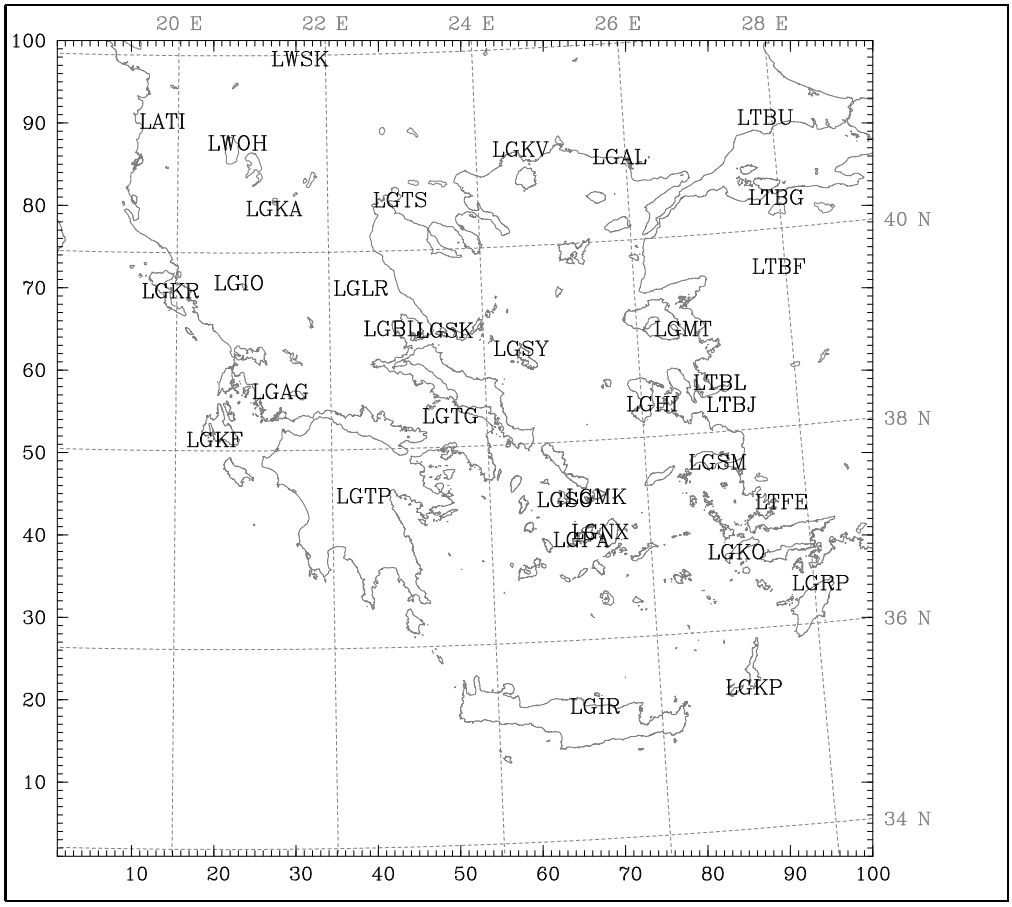

Fig. 2: *As in Fig. 1, but for domain 4.*

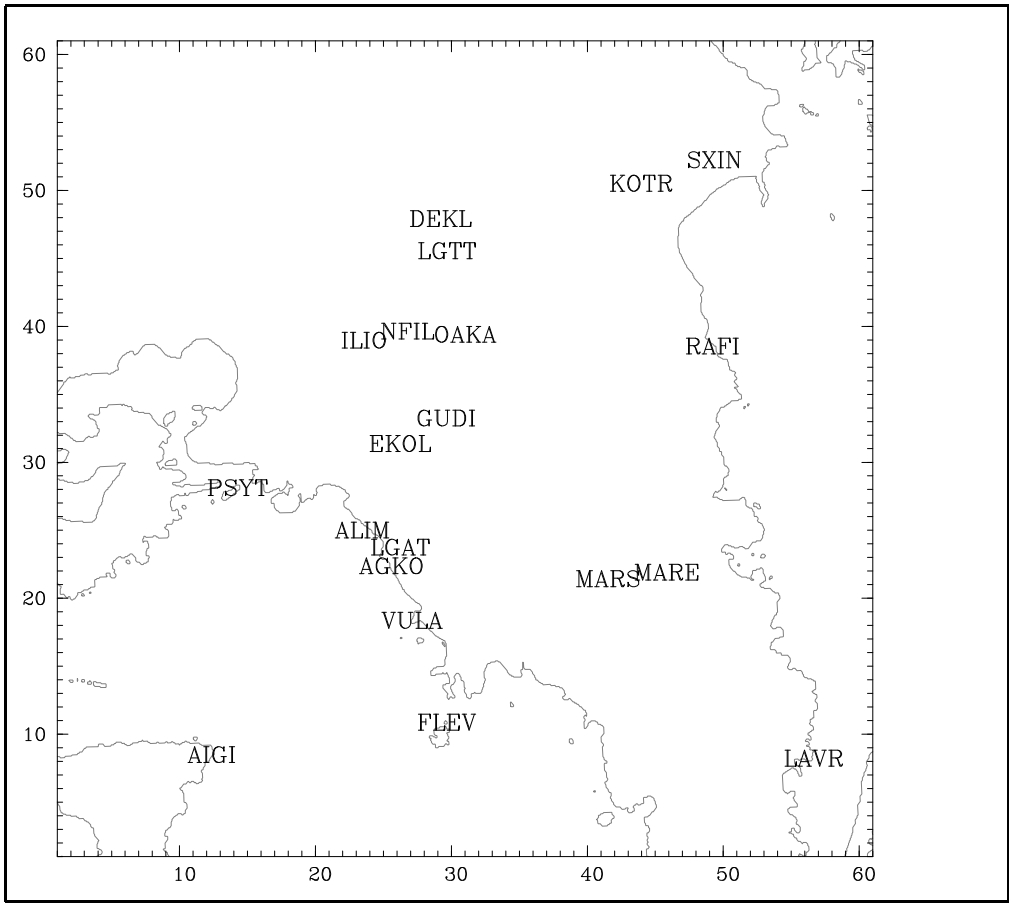

Fig. 3: *Mean 2-m temperature, 2-m dew point temperature and 10-m wind speed computed for the OGP from top of the hour observations. Values are plotted using the format: temperature/dew point temperature/wind speed. Observing sites are located where the dew point temperature is plotted. Shaded is model orography in metres.*

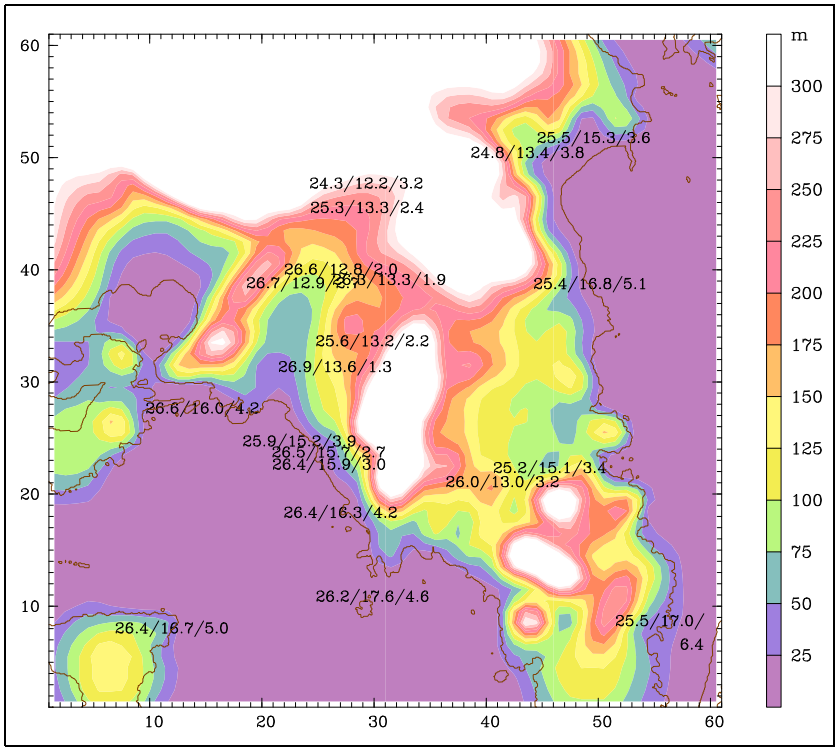

Fig. 4: *Placement of MM5 domains as configured for Olympic Games at HNMS.*

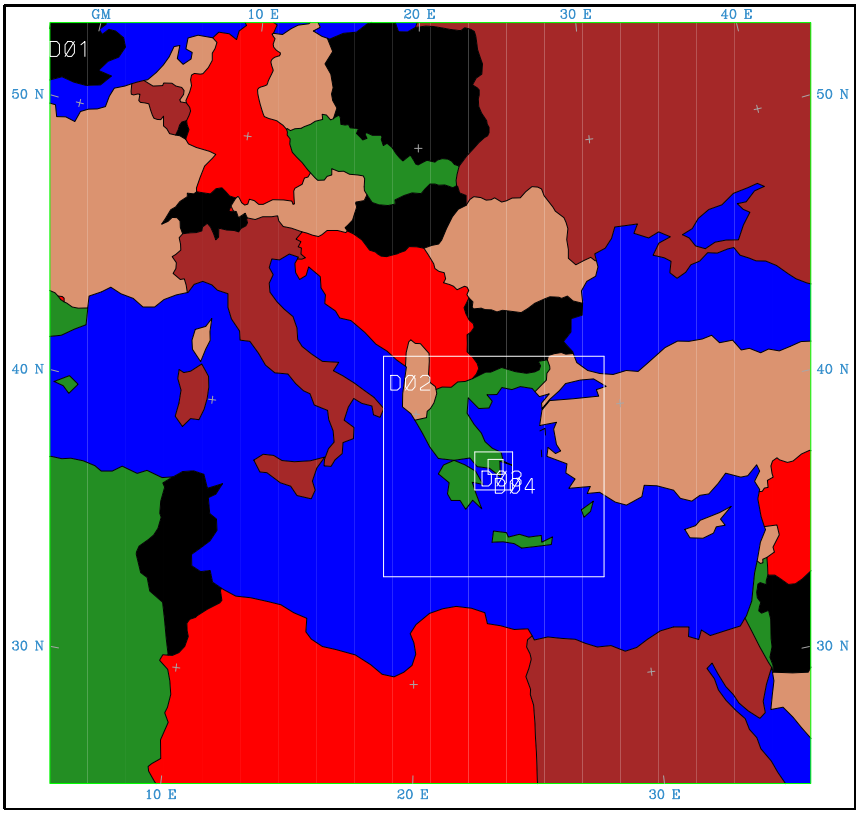

Fig. 5: *Example of nowcasting system graphic showing forecast of 2-m temperature (shaded, degrees C) and 10-m wind field (using standard notation of one barb=5* ms^{-1} *).*

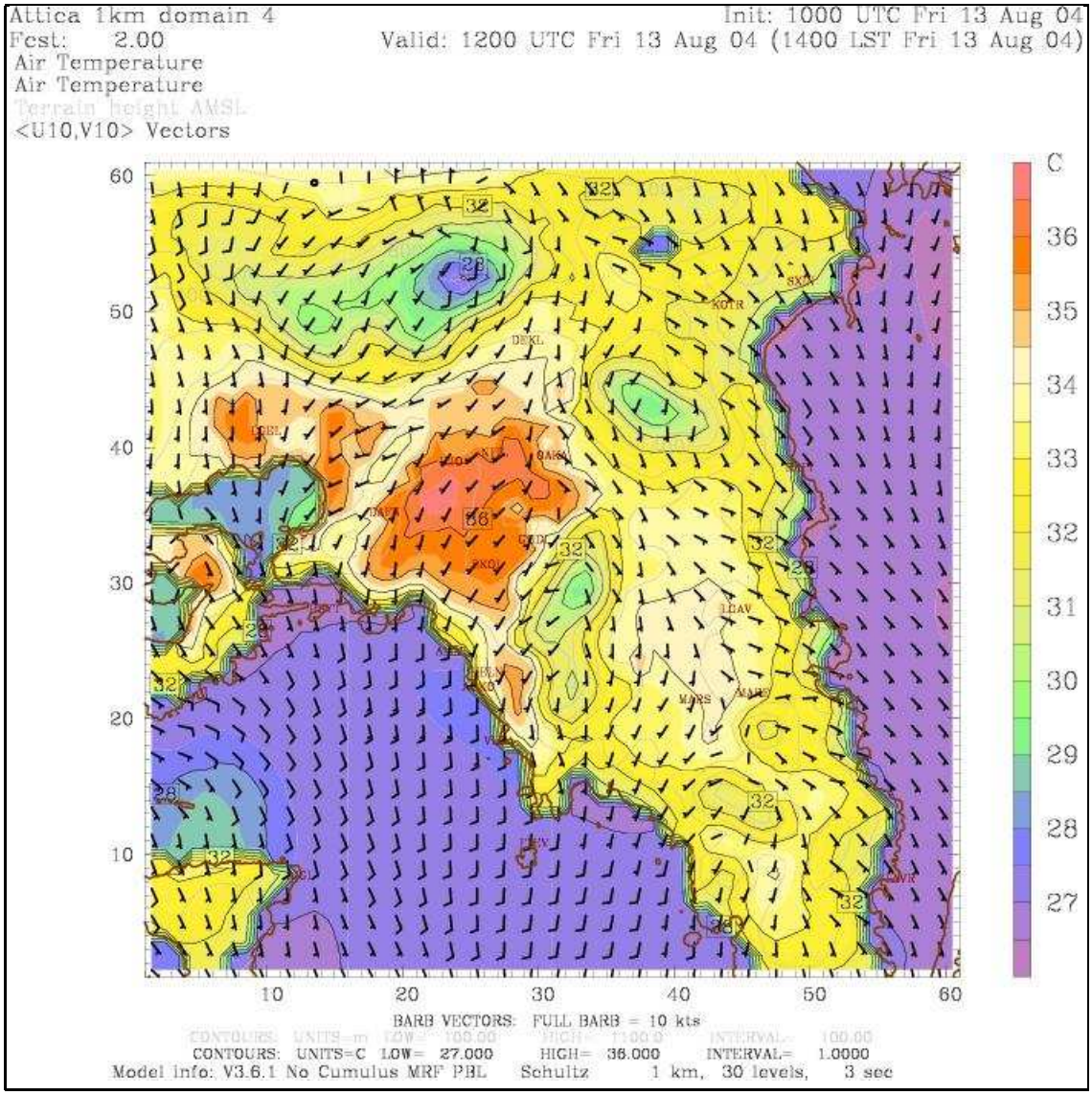

Fig. 6: *Domain 2 mean forecast error (forecast minus observed) by observation location for forecast lengths 2 through 8 h for a) 2-m temperature, b) 2-m dew point temperature and c) 10-m wind speed. Units are degrees Celsius, except* ms^{-1} *for wind speed.*

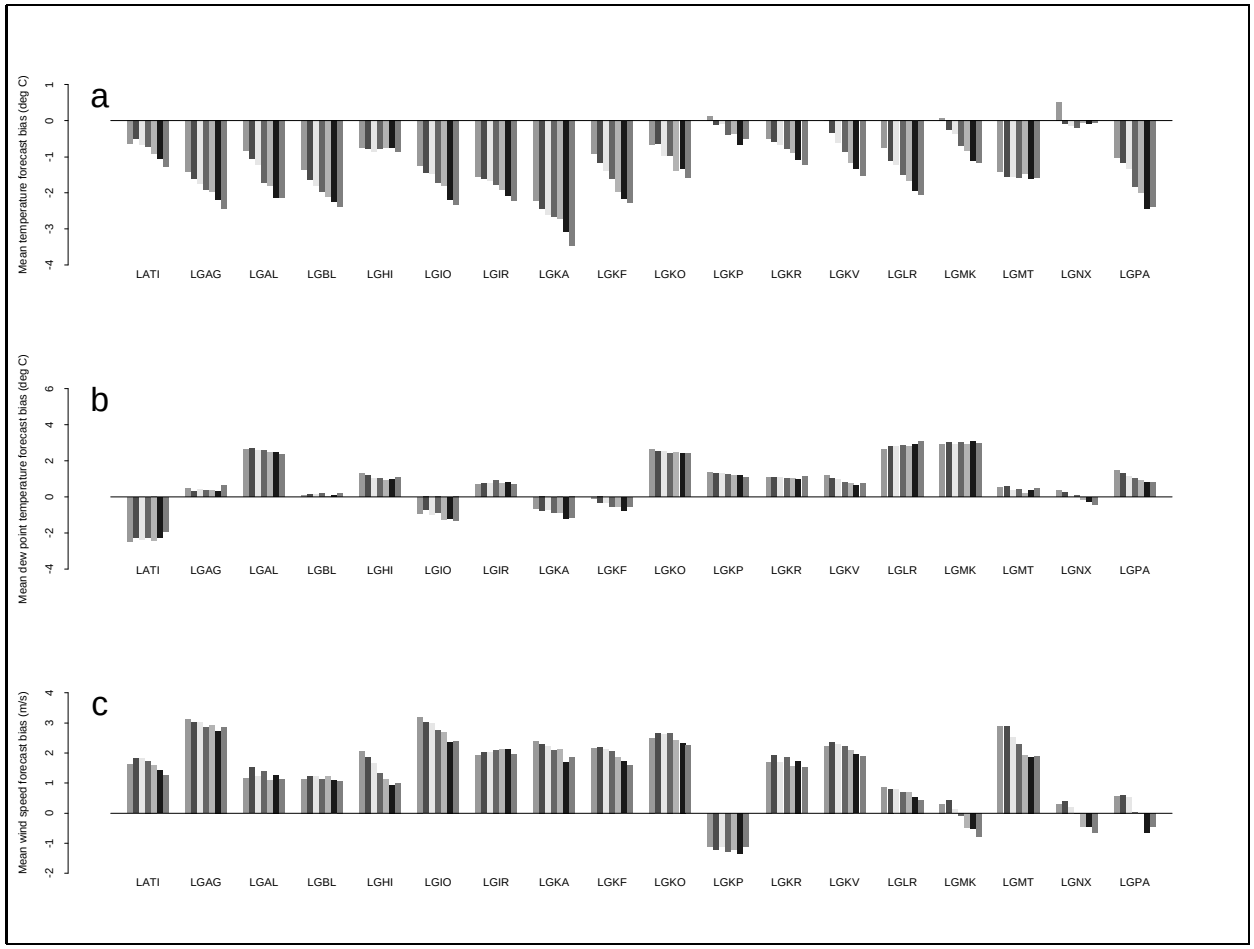

Fig. 7: *As in Fig. 6 except for different stations in domain 2.*

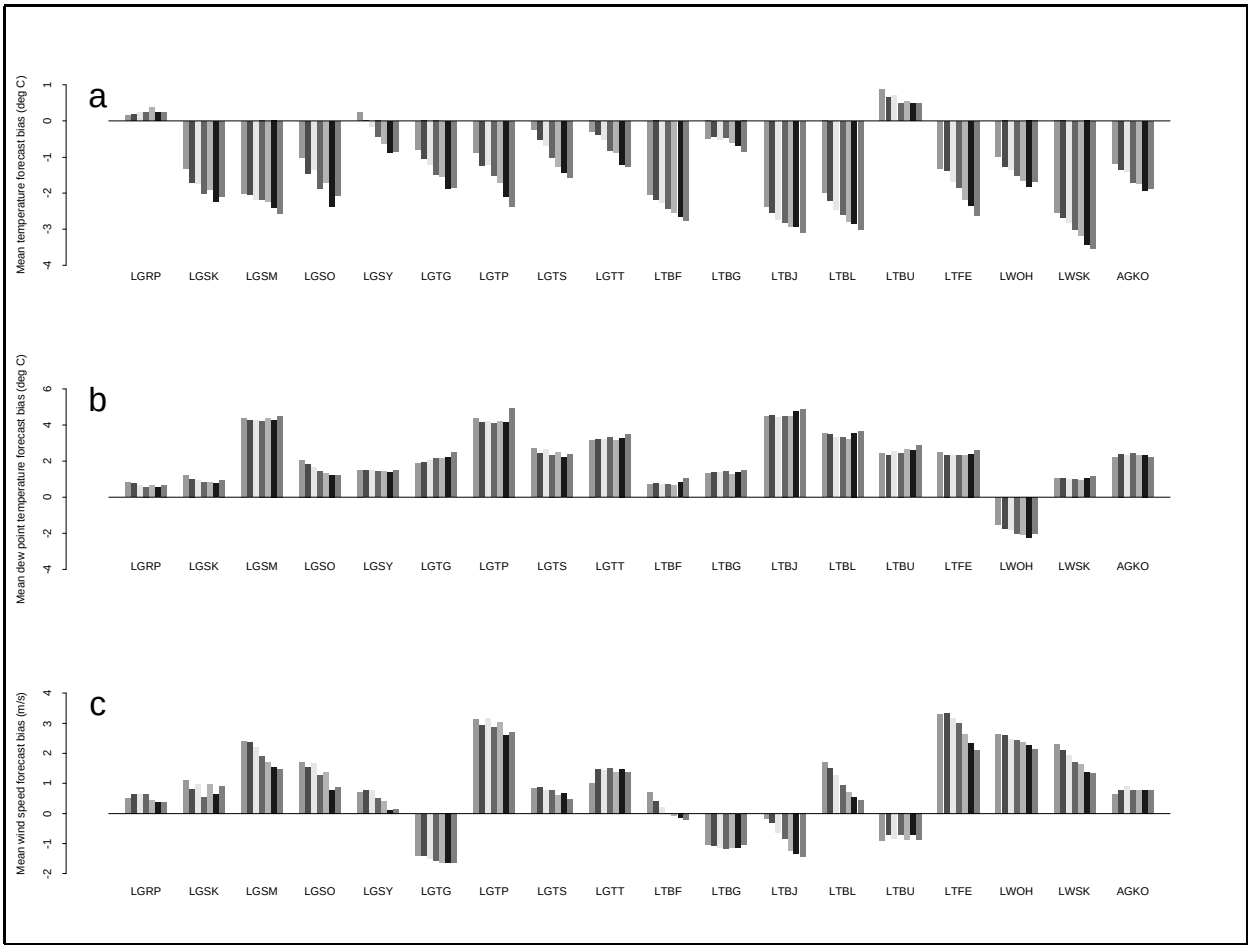

Fig. 8: *As in Fig. 6 except for different stations in domain 2.*

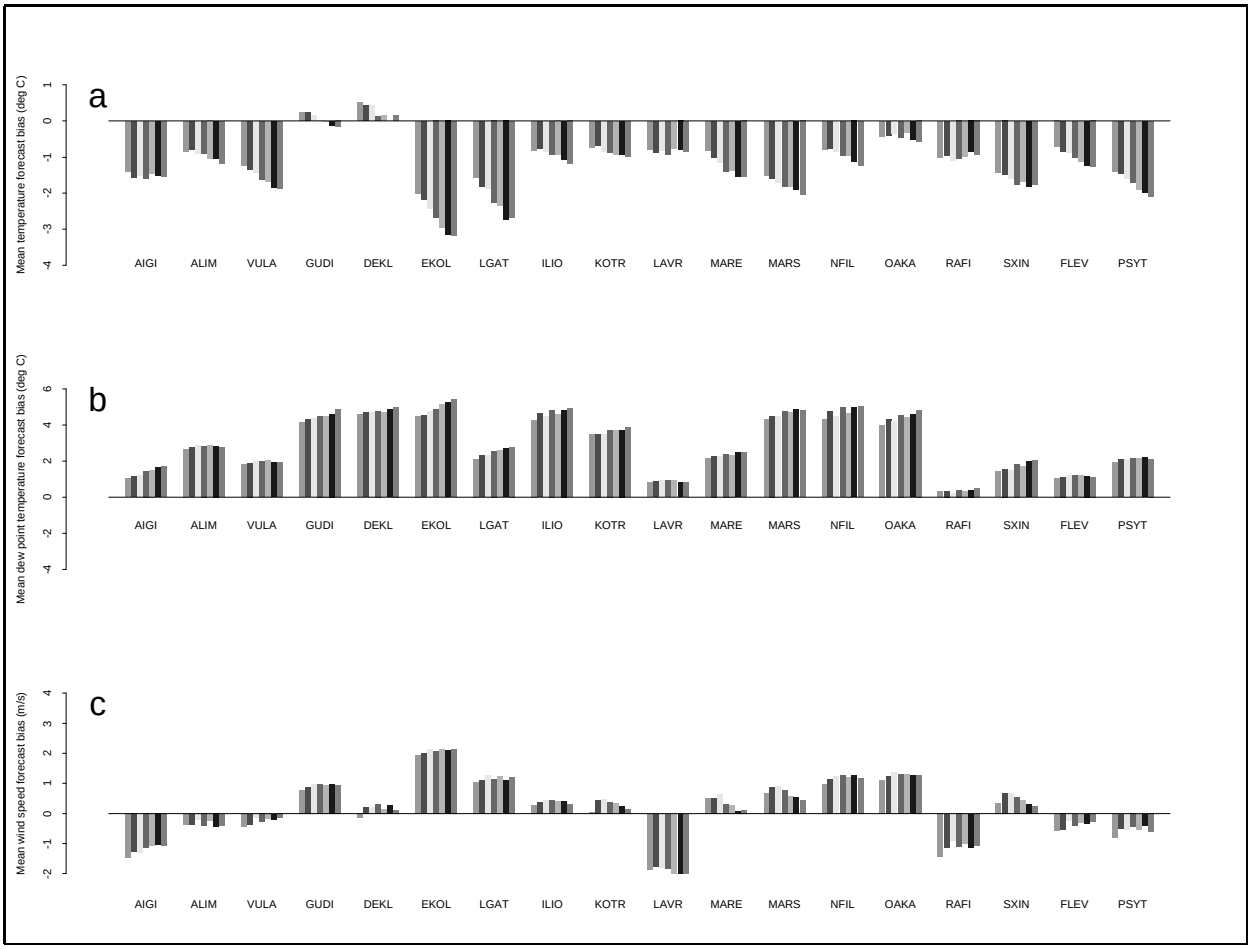

Fig. 9: *Hellenikon sounding valid 1200 UTC 18 August 2004 - the same time as in Fig. 5. Sounding courtesy of the University of Wyoming, USA.*

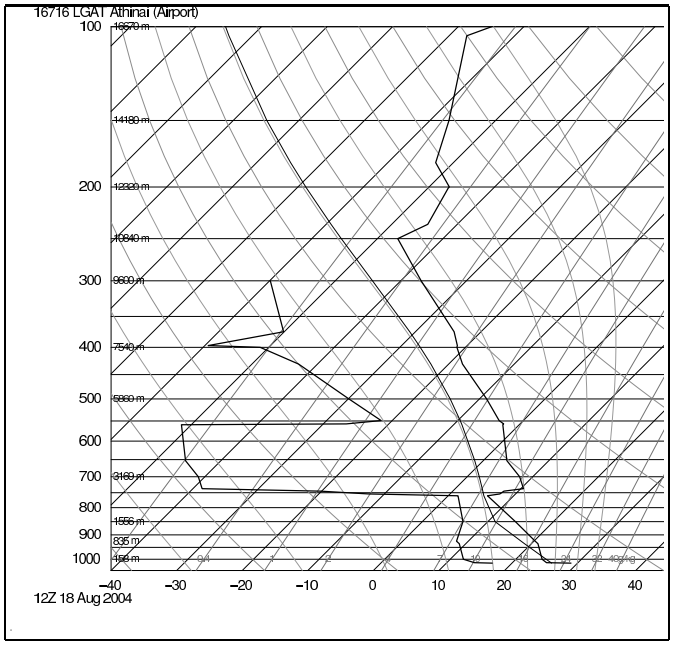

Fig. 10: *Domain 2 mean forecast error by valid time of observations for forecast lengths 2 through 8 h for a) 2-m temperature, b) 2-m dew point temperature and c) 10-m wind speed. Units are degrees Celsius, except* ms^{-1} *for wind speed. Note that observations valid on even (odd) numbered hours verify against forecast lengths 2, 4, 6 and 8 h (3, 5 and 7 h). Note nighttime sample sizes are limited by the availability of observations.*

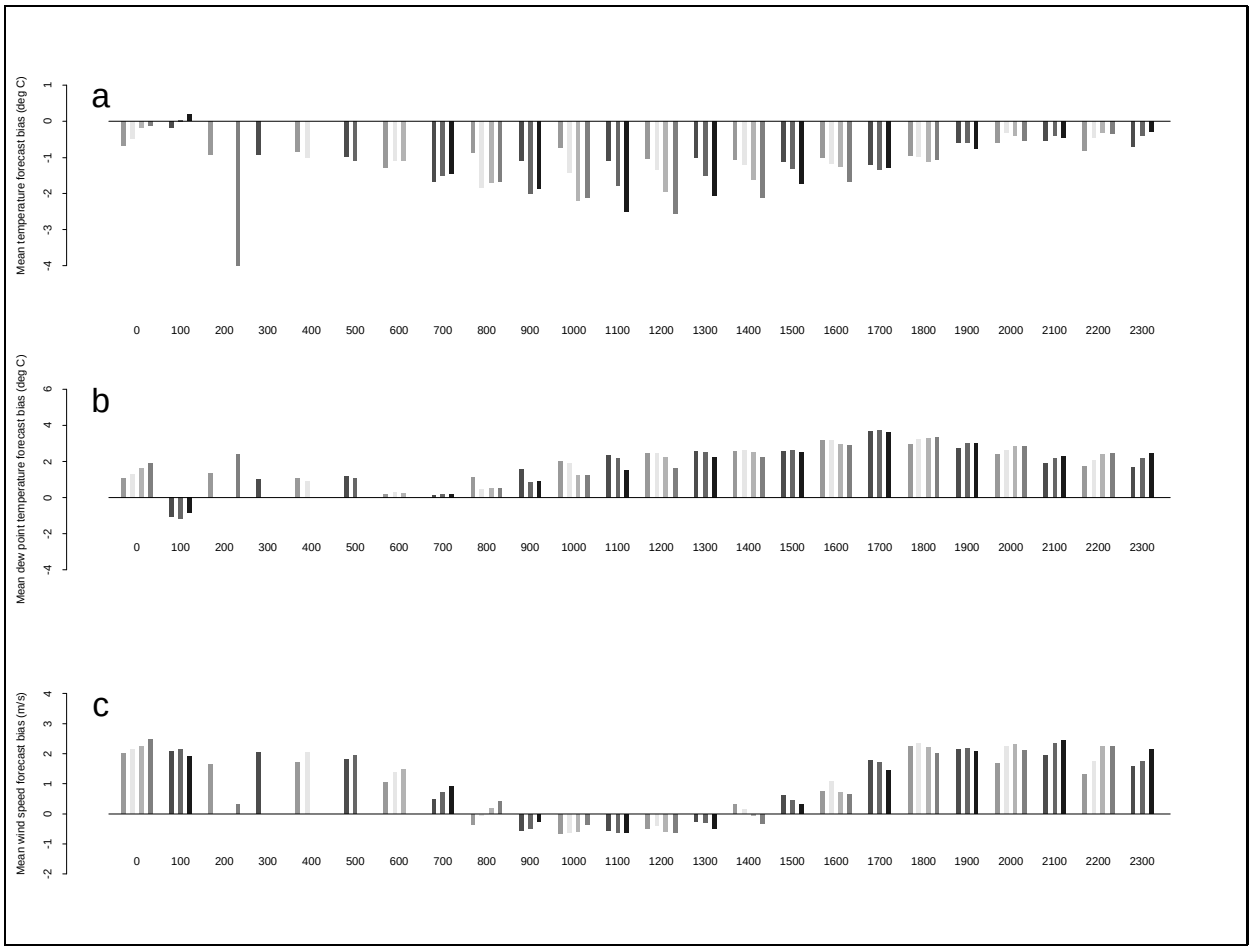

Fig. 11: *As in Fig. 6, except for domain 4.*

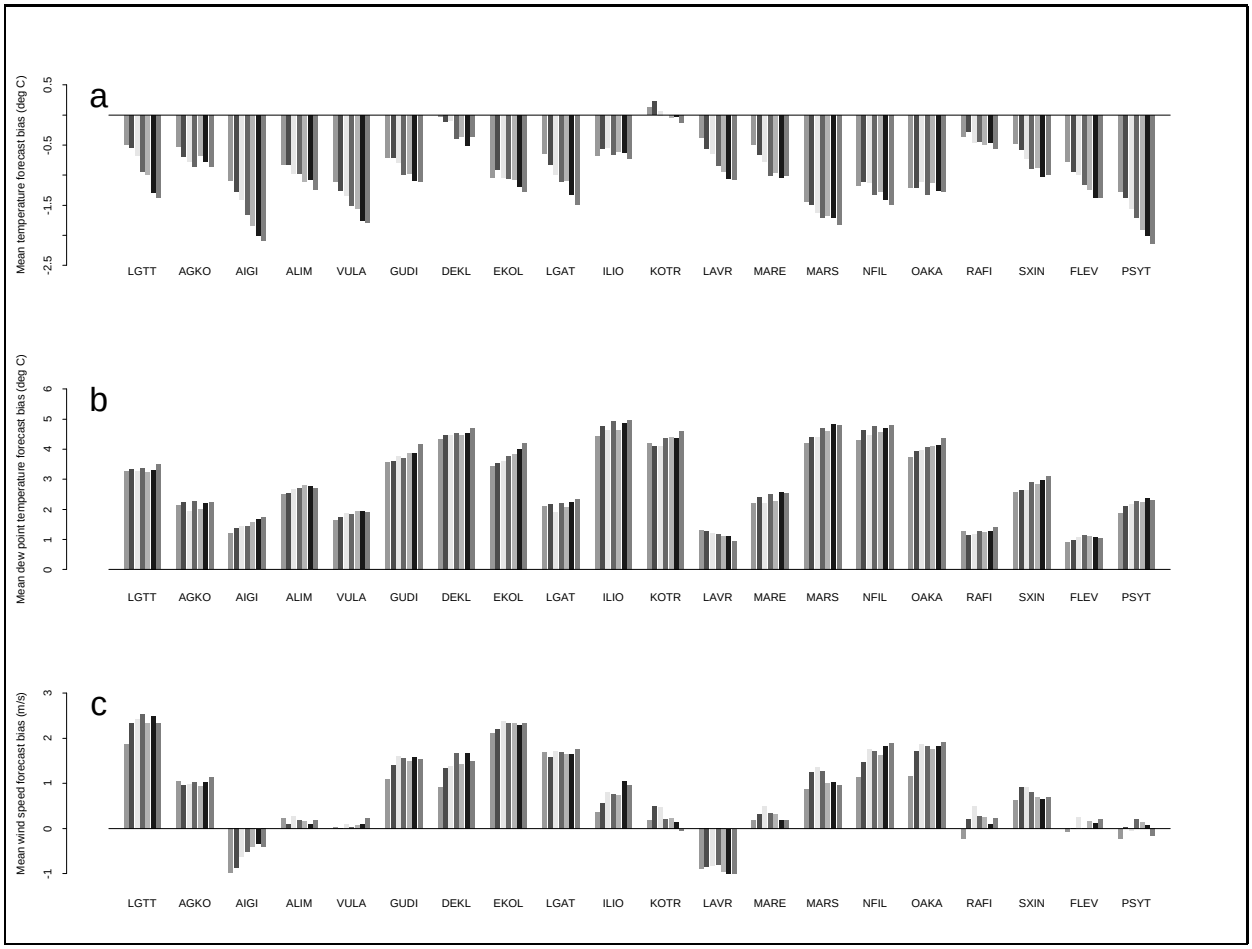

Fig. 12: *As in Fig. 10, except for domain 4.*

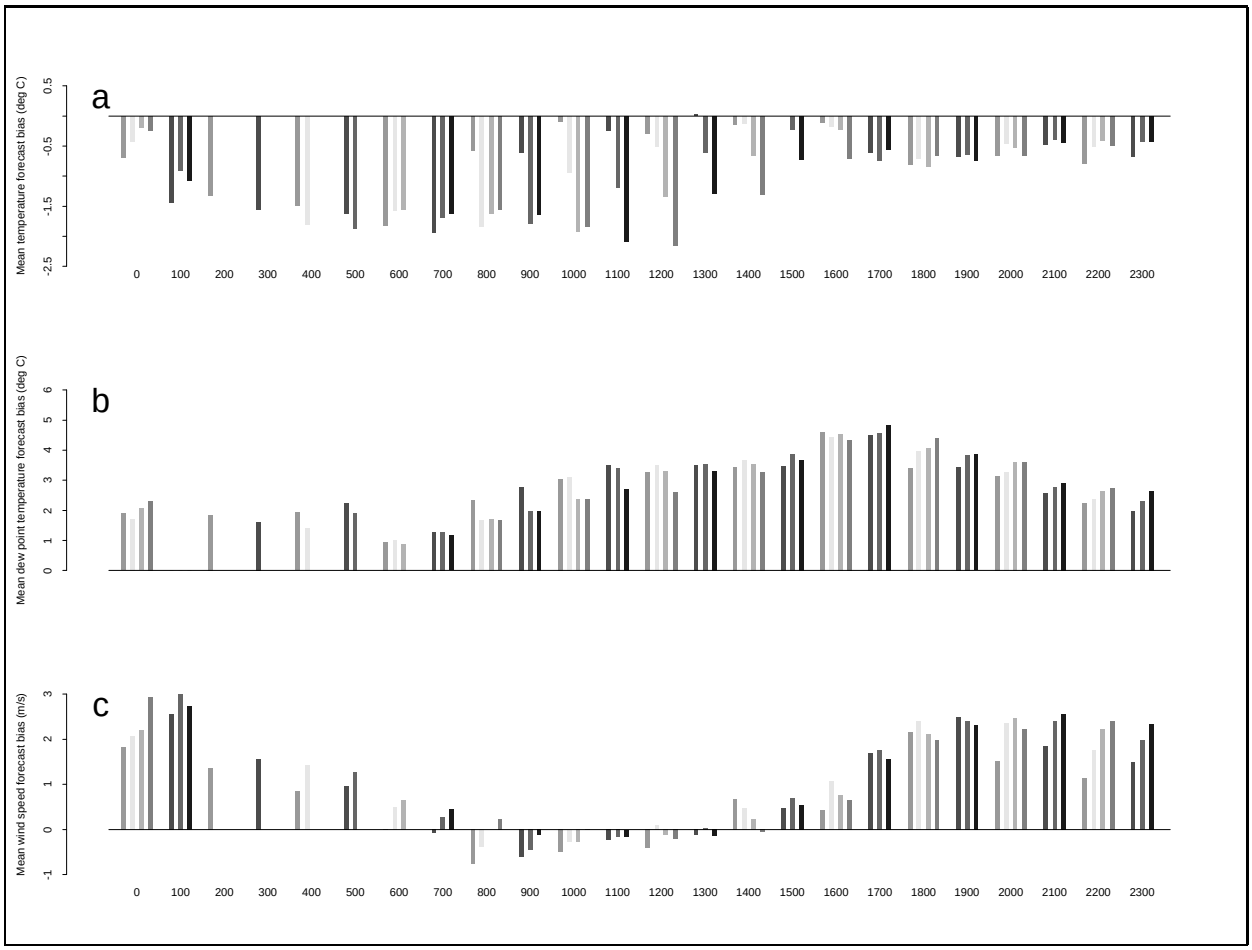

Fig. 13: *Example of spurious convection generated by the MM5. Shaded is 2-m relative humidity (%); the wind field is plotted using barbs in the conventional manner.*